Arabian Journal of Chemistry (2016) 9, S1962–S1972

King Saud University

Arabian Journal of Chemistry

www.ksu.edu.sa
www.sciencedirect.com

ORIGINAL ARTICLE

Ultrasound-assisted chiral derivatization of etodolac with (1*R*)-(−)-menthyl chloroformate for the determination of etodolac enantiomers

Yan Jin [a], Jing Zhao [a], Lydia Rhyman [b], Ponnadurai Ramasami [b], Yujin Shin [a], Kyung Min Jeong [a], Jeongmi Lee [a,*]

[a] *School of Pharmacy, Sungkyunkwan University, Suwon 16419, Republic of Korea*
[b] *Computational Chemistry Group, Department of Chemistry, Faculty of Science, University of Mauritius, Réduit 80837, Mauritius*

Received 29 July 2015; accepted 3 November 2015
Available online 11 November 2015

KEYWORDS

Enantiomeric separation;
Etodolac;
(1*R*)-(−)-menthyl chloroformate;
Fluorescence detection;
Response surface methodology;
Diastereomer.

Abstract This study presents the first report of an ultrasound-assisted derivatization reaction between a carboxylic acid of etodolac (ETO) and a chiral derivatization reagent, (1*R*)-(−)-menthyl chloroformate (*R*-MCF). Fifty μL of deproteinated mouse serum containing ETO enantiomers was derivatized with 125 μL of 200 mM *R*-MCF and 17 μL of pyridine (a catalyst), with the reaction facilitated by ultrasonic radiation for 13 min, which were the optimal conditions as determined by response surface methodology. After quenching the reaction by adding an aqueous L-proline solution, the mixture was subjected to salting-out assisted liquid–liquid extraction (SA-LLE), which provided phase separation for sample concentration as well as cleanup. The ETO diastereomers were separated on a Phenomenex Gemini C_{18} column (150 × 4.6 mm, 5 μm) under a simple gradient elution of a mobile phase containing a mixture of methanol: acetonitrile (10:1, V/V) and 10 mM acetic acid at a flow rate of 1.0 mL min^{-1}, followed by fluorescence detection with excitation and fluorescence emission wavelengths of 235 nm and 345 nm, respectively. The developed method was validated for specificity, sensitivity, linearity, accuracy, precision, stability, and matrix effect. A good linearity in the range of 0.5–50.0 μg mL^{-1} for each ETO enantiomer with $r^2 > 0.998$ and acceptable values for the intra-day and inter-day accuracy and precision

Abbreviations: ACN, acetonitrile; CDR, chiral derivatization reagent; CSP, chiral stationary phase; DFT, density functional theory; ETO, etodolac; FA, formic acid; FL, fluorescence; IS, internal standard; LOQ, limit of quantitation; MCF, menthyl chloroformate; NAP, naproxen; NSAID, nonsteroidal anti-inflammatory drug; QC, quality control; SA-LLE, salting-out assisted-liquid liquid extraction.

* Corresponding author. Tel.: +82 31 290 7784; fax: +82 31 292 8800.
E-mail addresses: jlee0610@skku.edu, jlee0610@gmail.com (J. Lee).

Peer review under responsibility of King Saud University.

Production and hosting by Elsevier

http://dx.doi.org/10.1016/j.arabjc.2015.11.001

as well as negligible matrix effects supported the suitability and reliability of the method. Finally, this method was used to analyze real samples taken from mice treated with (±)-ETO.

1. Introduction

More than half of the drugs in current use contain one or more chiral centers and are sold as either racemic mixtures or single enantiomers (Brocks, 2006; Awad and El-Aneed, 2013). Enantiomers of chiral drugs have identical physicochemical properties in achiral environments. However, they can have different pharmacodynamic, pharmacokinetic, and toxicological properties due to their different stereospecific interactions with endogenous molecules in chiral environments *in vivo* (McConathy and Owens, 2003; Smith, 2009; Shen et al., 2013; Tougou et al., 2004; Lu, 2007). Because distinct enantiomers should be considered as two separate drugs, they need to be evaluated separately (Hewala et al., 2014). Accordingly, the development of enantiomeric separation methods of racemic mixtures of drugs is important for drug monitoring (Burke and Henderson, 2002; Miller and Ullrich, 2008).

Many nonsteroidal anti-inflammatory drugs (NSAIDs) contain a chiral center, but they are usually sold as a racemic mixture (Evans, 1992). For example, etodolac (ETO), [(*RS*)-2-(1,8-Diethyl-4,9-dihydro-3*H*-pyrano[3,4-b]indol-1-yl) acetic acid], which was approved by the FDA for treating rheumatoid arthritis and osteoarthritis (Boni et al., 2000), has one chiral center. Although it is sold as a racemate, only *S*-ETO is responsible for anti-inflammatory activity, while *R*-ETO is useful in treating B-cell chronic lymphocytic leukemia and in reducing the adverse effects associated with the administration of the racemic mixture of ETO (Kolluri et al., 2005; Inoue et al., 2010; Hardikar, 2008). After administration, ETO does not undergo *in vivo* conversion between the *S*- and *R*-forms, and clearance of *S*-ETO is approximately 13 times faster than that of *R*-ETO, resulting in an effective 1:10 (*S*-) to (*R*-) physiological ratio in plasma (Hewala et al., 2014; Boni et al., 2000). Therefore, quantitative enantioseparation of ETO in biological samples is necessary for accurate determination of the differential potencies in pharmacological and toxicological aspects.

Similar to other enantiomers, chiral separation of ETO has been achieved through the formation of either transient or formal diastereomers (Stalcup, 2010). Although there have been a few studies based on capillary electrophoresis using chiral selectors (de Pablos et al., 2005; Fanali et al., 2003), high performance liquid chromatography (HPLC) analysis on a chiral stationary phase (CSP) using chiral columns has been the main stream approach for enantiomeric separation of ETO (Hewala et al., 2014; Becker-Scharfenkamp and Blaschke, 1993; Ali and Aboul-Enein, 2003; Ghanem et al., 2010; Caccamese, 1993), as chiral columns are convenient and do not raise the concern of racemization during analysis. However, some chiral columns are not commercially available (Boni et al., 2000) and are often of high costs (Ghanem et al., 2010). Columns are usually available in normal-phase mode, which requires the consumption of large volumes of volatile organic solvents as mobile phase (Hewala et al., 2014; Ghanem et al., 2010). These limit the practicality of CSP columns for chiral separation.

Formation of formal diastereomers of ETO has been achieved by chiral derivatization using a variety of chiral derivatization reagents (CDRs) including *S*-(+)-amphetamine sulfate (Singh et al., 1986) for gas chromatography, and (*S*)-1-(4-dimethylaminophenylcarbonyl)-3-aminopyrrolidine (Ogawa et al., 2013), (*S*)-anabasine Higashi et al., 2012, *S*-(−)-1-(1-naphthyl)-ethylamine (Jin et al., 2008), (*R*)-(+)-α-methyl benzyl amine, (*S*)-(−)-α,4-dimethylbenzylamine, and (*R*)-(−)-1-cyclohexylethylamine (Singh and Bhushan, 2015) for HPLC analysis. These CDRs display some disadvantages, including the lengthy derivatization times required (Singh et al., 1986; Jin et al., 2008), commercial unavailability (Ogawa et al., 2013), or high costs (Higashi et al., 2012). Only a small number of studies were developed for the ETO analysis in biological samples (Singh et al., 1986; Jin et al., 2008), while several methods were not validated appropriately (Higashi et al., 2012). Therefore, the development of indirect methods involving CDRs that are more economical and readily available and that can produce stable products under mild conditions remains necessary.

In this study, we aimed to develop a new analytical method for the simple and sensitive determination of ETO enantiomers in biological fluids. To this end, (1*R*)-(−)-menthyl chloroformate (*R*-MCF) was selected as the most appropriate CDR. *R*-MCF has been widely used for enantiomeric separation of chiral drugs that contain amino or hydroxyl groups by forming stable derivatives (Christensen et al., 1995; Koo et al., 2012; Paik et al., 2006; Kino et al., 2004). This study presents the first use of *R*-MCF as a CDR to react with a carboxylic acid group of ETO. The derivatization reaction was facilitated efficiently by ultrasound radiation and the reaction conditions including the radiation time and the CDR volume were optimized by response surface methodology (RSM). Fluorescence (FL) detection of the ETO diastereomers, which was possible due to the native fluorescent property of ETO (El Kousy, 1999), allowed for sensitive and selective analysis by HPLC compared to ultraviolet detection. The validity of the developed method was demonstrated by the reasonably acceptable parameters of the method validation, and by its successful application to real serum samples taken from mice that had been administered a racemic mixture of ETO.

2. Materials and methods

2.1. Materials

(±)-ETO (>98.0%) was obtained from TCI (Tokyo, Japan). *R*-MCF (>99.0%), pyridine, acetic acid, formic acid (FA), L-proline, and *S*-naproxen sodium (*S*-NAP; >98%) were purchased from Sigma–Aldrich (St. Louis, MO, USA). Ethanol (EtOH) and sodium chloride (NaCl) were purchased from Merck (Darmstadt, Germany). HPLC-grade water, methanol (MeOH), and acetonitrile (ACN) were obtained from J.T. Baker (Center Valley, PA, USA). A few lots of mouse serum, each of which was a pooled preparation from a normal mouse population and pooled for the method development and validation processes, were purchased from Sigma–Aldrich. Other chemicals were of analytical grade and purchased from Sigma–Aldrich unless otherwise indicated.

2.2. Instruments and operation conditions

2.2.1. HPLC–FL analysis of ETO diastereomers for quantitative assays

Quantitative chromatographic analyses were performed on an Agilent Technologies 1260 Infinity Liquid Chromatographic System (Agilent Technologies, Santa Clara, CA, USA) equipped with a G1311C Quaternary Pump VL, a G1316A Thermostatted Column Compartment, and a G1321B fluorescence detector. For fluorescence detection, the excitation and emission wavelengths were set at 235 and

345 nm, respectively. The injection volume was 20 μL and the chromatographic separation was performed on a Phenomenex Gemini C_{18} column (150 mm × 4.6 mm, 5 μm) at a flow rate of 1 mL min^{-1} at 45 °C. The mobile phase consisted of eluent A (10 mM acetic acid) and eluent B (MeOH: ACN, 10:1 v/v). The gradient elution was performed as follows: 0–10 min, 80–85% B; 10–15 min, 85% B; 15–20 min, 85–90% B. After the gradient was returned to the initial conditions within 3 min, the column was re-equilibrated for 5 min before the next run.

HPLC–UV analysis, which was used to compare method sensitivity of the HPLC–FL analysis, was performed using a PerkinElmer LC system (Norwalk, CT, USA), equipped with a PerkinElmer micro pump, a column oven (series 200), an auto-sampler (series 275), and a photodiode array detector (series 275). The system operation and data management were conducted using TotalChrom Workstation software. Detection wavelength was set at 226 nm and the other chromatographic conditions were the same as for the HPLC-FL analysis.

2.2.2. UHPLC–QTOF–MS analysis of ETO diastereomers for qualitative assays

Ultra-high performance liquid chromatography–quadrupole-time-of-flight mass spectrometry (UHPLC–Q-TOF–MS) was used for the qualitative analysis of ETO diastereomers. The instruments employed were an Acquity UPLC system (Waters Co., Milford, MA, USA) coupled to a Waters Acquity Xevo G2 Q-TOF system (Waters Corp., Manchester, UK), which had been used in our previous study (Nam et al., 2015). Overall, the operation conditions were similar to the previous study with slight modifications. In brief, separation was achieved on a ZORBAX Rapid Resolution High Definition Eclipse Plus C_{18} column (100 mm × 2.1 mm, 1.8 μm) from Agilent under a simple gradient elution of the mobile phase consisting of 0.1% FA in water (A) and 0.1% FA in MeOH (B): 0–9 min, 80–90% B; 11–13 min, 100% B. Mass spectrometry was conducted in positive ion mode and other MS parameter settings were the same as those in Nam et al. (2015).

2.3. Preparation of standard and reagent solutions

A standard stock solution of racemic ETO was prepared at a concentration of 1000.0 μg mL^{-1} in ACN. Standard working solutions were prepared in the range of 1.0–100.0 μg mL^{-1} by subsequently diluting the stock solution in ACN. Stock solution and working solution of *S*-NAP, the internal standard (IS), were prepared in EtOH. All standard working and stock solution were stored at −20 °C until use. The derivatization reagent, 200 mM *R*-MCF, was prepared in ACN and stored at 4 °C.

2.4. Chiral derivatization reaction procedure

Equal volumes of ETO working solution and mouse serum were combined to yield 100 μL of a mixture which was then spiked with 20 μL of a 1.0 μg mL^{-1} solution of *S*-NAP. After 880 μL of ACN was added to precipitate protein, the mixture was vortexed for 3 min and centrifuged at 12,300 *g* for 5 min. A total of 950 μL of the supernatant was removed and dried under nitrogen gas purge. The residues were derivatized as follows: 125 μL of 200 mM *R*-MCF, 58 μL of ACN, and 17 μL of pyridine were added, and the reaction mixture was capped, followed by ultrasonic radiation for 13 min. The reaction was quenched by the addition of 170 μL of 200 mM L-proline solution and subsequently vortexed for 3 min followed by incubation at room temperature for 10 min. Phase separation was readily achieved by the addition of 20 mg of NaCl to the reaction mixture and subsequent brief vortexing. The upper organic phase of 140 μL was removed and filtered through 0.45 μm pore membrane filters (Millipore, Tullagreen, Ireland) before injection into the HPLC system.

2.5. RSM for the optimization of derivatization conditions

RSM based on a central composite design was performed using Design-Expert 8 (Stat-Ease Inc., Minneapolis, MN, USA). The optimized variables were as follows: (1) A, volume of 200 mM *R*-MCF, (2) B, ultrasonic radiation time, and (3) C, pyridine volume. The total sum of two peak areas of derivatized ETO diastereomers was used as the response.

2.6. Assessment of the derivatization reaction rate

The derivatization reaction products of *R*- and *S*-ETO were examined for 0–20 min of ultrasonic radiation. The reaction conditions were based on the optimized conditions except for the reaction time. The total peak areas of the *R*- and *S*-ETO derivatives were used for the total reaction yields. Enantiomeric fractions (EFs) were measured for the *R*-ETO derivatives using the following equation (Polo-Diez et al., 2015; Ribeiro et al., 2014):

$$\textit{Enantiomaric fraction } (EF) = \frac{\text{peak area of } R \text{ enantiomer}}{\text{peak area } R \text{ enantiomer} + \text{peak area of } S \text{ enantiomer}}.$$

2.7. Density functional theory method for computing dipole moment of derivatives

A computational study using density functional theory (DFT) was performed to compute dipole moment of the ETO derivatives. The old, but popular B3LYP (Becke, 1993; Lee et al., 1988) functional, and the more recent M06-2X (Zhao and Truhlar, 2008) functional were considered. The basis set used for all atoms was 6-31G(d) (Hehre et al., 1986). All computations were performed using Gaussian09 (Frisch et al., 2009). The diastereomers, *R*-ETO:*R*-MCF and *S*-ETO:*R*-MCF were fully optimized in MeOH and ACN as the solvents. Solvent effects were taken into account in the framework of self-consistent reaction field (SCRF) (Cances et al., 1997; Cossi et al., 1996; Barone et al., 1998) based on Polarizable Continuum Model (PCM) as developed by Tomasi's group (Tomasi and Persico, 1994). Frequency computations were performed on the optimized diastereomers using the same methods as for the optimization to check the nature of the stationary points.

2.8. Method validation

The established method was validated with respect to its constituent parameters according to the United States Food

and Drug Administration bioanalytical method validation guideline (Food and Drug Administration, 2001).

2.8.1. Specificity and sensitivity

Specificity was evaluated by comparing the chromatogram of the blank serum sample with that of the serum sample spiked with ETO and IS. Sensitivity was evaluated in terms of the limit of quantitation (LOQ), which was determined based on the determined analyte concentration at which the signal-to-noise ratio was greater than 10.

2.8.2. Linearity

Calibration curves for *R*- and *S*-ETO were established by spiking racemic ETO into blank serum at 1.0, 2.0, 5.0, 10.0, 20.0, 50.0, and 100.0 μg mL^{-1}, which correspond to 0.5, 1.0, 2.5, 5.0, 10.0, 25.0, and 50.0 μg ml^{-1} respectively, of each individual *R*- or *S*-ETO enantiomer.

2.8.3. Precision and accuracy

Precision and accuracy were evaluated using quality control (QC) samples that had been prepared by spiking ETO into blank sera at three different concentrations (0.5, 5.0, and 50.0 μg mL^{-1} for each enantiomer). The accuracy of the method was expressed as the percentage of the observed concentration obtained from the calibration curves relative to the predicted concentration. The precision was calculated as the relative standard deviation (% RSD). Intra-day assay precision and accuracy were assessed by analyzing the QC samples in five replicates on the same day. Inter-day precision and accuracy were evaluated by analyzing the QC samples in three replicates on three successive days.

2.8.4. Autosampler stability

The autosampler stability of the ETO derivatives in the prepared samples was monitored at three concentrations (0.5, 5.0, and 50.0 μg mL^{-1} for *R*- and *S*-ETO) at different time intervals. Nine samples were prepared at once, three of which were analyzed immediately ($t = 0$ h), while the remaining samples were stored at 4 °C and analyzed after 24 h ($n = 3$) and 48 h ($n = 3$) of storage. The relative deviations from the initial concentration after 24 and 48 h were calculated.

2.8.5. Matrix effects

Matrix effects were assessed in the following two methods. First, matrix-free standard solutions were prepared in ACN at the same concentration levels as used for the calibration curves prepared in serum matrices. The slopes of the external standard curves were compared to those of the standard addition curves. In the second method, the signals of the QC samples prepared in serum and the matrix-free samples prepared in ACN were compared at three concentrations level ($n = 3$). Peak area ratios of *R*- and *S*-ETO to IS in ACN and serum were measured, and the matrix effects were calculated using the following equation (Sergi et al., 2013; Chow et al., 2011):

$$\text{Matrix effect} = \frac{\text{peak area ratio in serum} - \text{peak area ratio in ACN}}{\text{peak area ratio in ACN}}.$$

2.9. Animal test for real sample analysis

Eight-week-old male ICR mice were purchased from Koatech Co., Ltd (Seoul, Korea). All animal care procedures were conducted in accordance with the US National Institutes of Health Guide for the Care and Use of Laboratory Animals. The procedures were reviewed and approved by the Institutional Animal Care and Use Committee of the School of Pharmacy, Sungkyunkwan University (Approval No. SKKUIACUC-20150034). A single dose of ETO racemates at 20 mg kg^{-1} was administered via intraperitoneal injection, and serum was collected 30 and 60 min after administration.

3. Results and discussion

3.1. Derivatization of ETO using *R*-MCF, and characterization of its reaction chemistry

Chloroformates can react with aliphatic alcohols, amines, and carboxylic acids to form carbonates, carbamates, and esters, respectively (Matzner et al., 1964; Lee et al., 2014). These facts suggest that both the secondary amine and the carboxylic acid group of ETO are the functional groups capable of reaction with *R*-MCF (Matzner et al., 1964). Pyridine has been used as a catalyst and scavenger of the hydrogen chloride formed during the derivatization reaction of chloroformates with amines and carboxylic acids (Lee et al., 2014; Farsam et al., 1999).

Based on the above facts, we examined the derivatization reactions between ETO racemates and *R*-MCF with and without the addition of pyridine. The multiple conjugated structure of ETO enables its detection by fluorescence emission (El Kousy, 1999) and ultraviolet absorption (Helmy and El-Bedaiwy, 2014). In this study, we used an FL detection system to attempt to selectively and sensitively detect ETO and its derivatives. For quantification, enantiomerically pure *S*-NAP, which is an NSAID with a carboxylic acid moiety and that possesses a native fluorescent property, was used as the IS.

First, derivatization was performed using 200 μL of 20 mM *R*-MCF in the absence of pyridine. As a result, the intact ETO peak was decreased, while no new peak was detected in the chromatogram of HPLC–FL analysis (Supplementary Fig. S1). On the other hand, UHPLC–Q-TOF–MS analysis of the derivatization products displayed one new peak, which had not been visible by the FL detection, in addition to the native ETO peak, which decreased. The accurate masses of the molecular ion and its fragment ions revealed that the new peak corresponded to a carbamate derivative of ETO formed between the indole amine of ETO and *R*-MCF (Table 1 and Supplementary Fig. S2). The ETO diastereomeric derivatives could not be resolved using a typical reversed phase C_{18} column in the UHPLC system. It is likely that the menthyl group attached directly on the indole amine induced fluorescence quenching in the ETO moiety. Thus, we concluded that the *R*-MCF derivatization without pyridine was inapplicable for producing ETO diastereomers suitable for enantioseparation using HPLC–FL.

In contrast, pyridine added to the derivatization reaction at a volume of 30 μL yielded very different results. The native ETO peak was decreased, and two incompletely resolved peaks were found to elute later in the HPLC–FL chromatogram under a simple gradient elution with an aqueous MeOH

Table 1 MS data for the *R*-MCF derivatives.

Analyte	Elemental composition	Exact mass	Measured mass	Mass error (ppm/mDA)	Mass fragment
ETO carbamate derivative[a]	$C_{28}H_{39}NO_5$	492.2726 ($[M+Na]^+$)	492.2719	−1.4/−0.7	270.1486, 228.1379
ETO ester derivative[b]	$C_{27}H_{39}NO_3$	426.3008 ($[M+H]^+$)	426.3007	−0.2/−0.1	288.1597, 172.1123
IS ester derivative[c]	$C_{24}H_{32}O_3$	391.2249 ($[M+Na]^+$)	391.2243	−1.5/−0.6	231.1017, 185.0960

[a] Peak 1 in Fig. 1.
[b] Peaks 2 and 3 in Fig. 1.
[c] Peak 4 in Supplementary Fig. S1.

mixture (data not shown). Based on the UHPLC–Q-TOF–MS analysis of the reaction products, it was confirmed that the two peaks were ETO ester diastereomers that had been produced by the reaction of *R*-MCF with the carboxylic acid group of ETO (Table 1 and Supplementary Fig. S2). Fluorescence of the derivatives produced in the presence of pyridine yielded levels similar to that of the native ETO under the same detection conditions. Accordingly, we used the same excitation and emission wavelengths for the derivatives as for native ETO, with which the peak of *S*-NAP diastereomer also yielded a signal similar to that of the native *S*-NAP. The two derivatization reactions, differing according to the presence of pyridine, are shown in Fig. 1.

3.2. Chromatographic resolution of the ETO diastereomers

Since diastereomers have very similar but not identical chemical and physical properties, they can be resolved on conventional achiral columns. In our initial study, the two diastereomeric derivative peaks were not completely resolved and an interfering endogenous peak slightly overlapped with the peak of the second diastereomer that eluted under the aqueous MeOH solution gradient. Accordingly, we attempted to optimize the chromatographic conditions to achieve improved resolution of these overlapping peaks.

To this end, we investigated the effects of the properties of aqueous and organic solvents in the mobile phase, and of

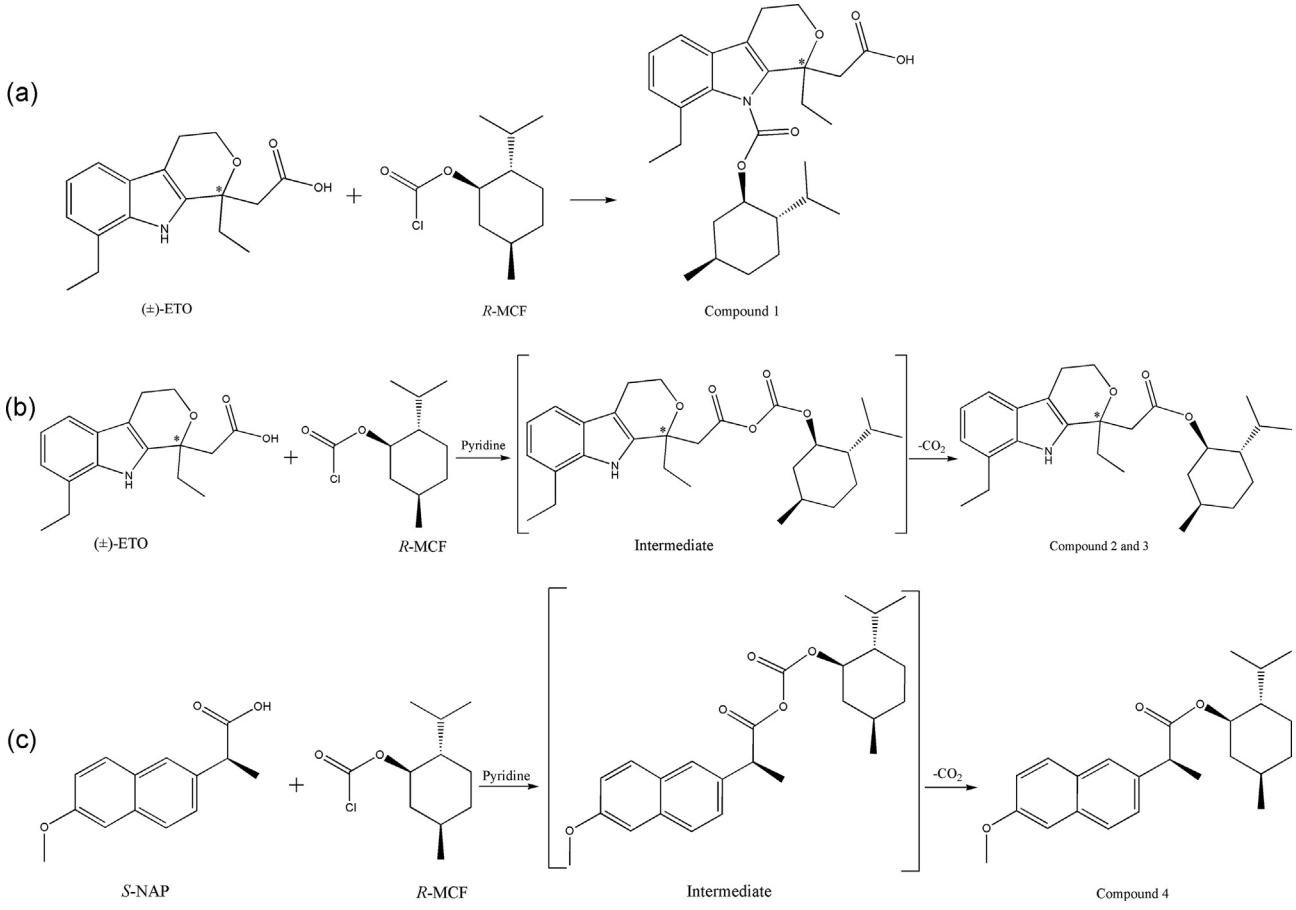

Figure 1 Schemes for the derivatization reactions with *R*-MCF. (a) ETO derivatization in the absence of pyridine, (b) ETO derivatization in the presence of pyridine, and (c) IS (*S*-NAP) derivatization in the presence of pyridine. The asterisk indicates a chiral center.

Table 2 Electric dipole moment (Debye) of the two fully optimized diastereomers using B3LYP/6-31G(d) and M06-2X/6-31G(d) methods in MeOH and ACN.

Method	*R*-ETO diastereomer	*S*-ETO diastereomer
MeOH		
B3LYP/6-31G(d)	6.97	6.67
M06-2X/6-31G(d)	7.16	6.63
ACN		
B3LYP/6-31G(d)	6.99	6.68
M06-2X/6-31G(d)	7.17	6.64

column temperature, while modifying gradient elution conditions as appropriate. First, we found that changing the mobile phase component from water to 10 mM acetic acid as eluent A yielded a baseline separation of the two ETO diastereomers. However, the problem of the second diastereomer peak overlapping with the following impurity peak still remained. Thus, we changed the organic solvent of the mobile phase from MeOH to ACN, which resulted in a distinct separation between the second diastereomer and the interfering peaks, although the two ETO diastereomers could not be separated at baseline. We then combined MeOH and ACN at various ratios, and found that a mixture of MeOH and ACN at 10:1 (v/v) yielded baseline separation of the two diastereomers and impurity peaks (data not shown). All of these modifications were performed at a column temperature 25 °C. Finally, the effect of column temperature was examined, varying from 25 °C to 45 °C. It was found that the shortest run time without compromising resolution was achieved at 45 °C, which was accordingly selected as the column temperature for the final chromatographic conditions as described in Section 2.2.1. The total chromatographic run time was 23 min.

3.3. Differentiation between R- and S-ETO diastereomers by in vivo assay and computational study

Direct identification of the *R*- and *S*-ETO diastereomers was not achievable because enantiomerically pure ETO standards could not be obtained. Nonetheless, resolution of the *R*- and *S*-ETO is still meaningful as previously reported (Higashi et al., 2012; Singh and Bhushan, 2015). Differentiation between the two diastereomers was inferred from *in vivo* assay results. Serum samples taken from ICR mice 30 min and 60 min after administration of (±)-ETO were prepared using the initial derivatization conditions involving pyridine, and were promptly analyzed by HPLC–FL. Based on previous stereoselective pharmacokinetic studies of ETO that showed a predominant chiral disposition of the *R*-form *in vivo* due to the rapid metabolism of the *S*-form (Boni et al., 2000; Brocks and Jamali, 1990), we concluded that the first eluting diastereomer peak (peak 2), which was always much larger than the second peak (peak 3), was the *R*-ETO diastereomer, followed by the second peak, corresponding to the *S*-ETO diastereomer (Supplementary Fig. S3).

To complement our experimental investigations, we also performed a computational study using DFT to compute dipole moment, which is a useful parameter to understand the order of elution in LC. The coordinates of the optimized structures of the two diastereomers, *R*-ETO:*R*-MCF and *S*-ETO:*R*-MCF, are given in Supplementary Table S1. The electric dipole moments of the two fully optimized diastereomers are summarized in Table 2. As per the experimental conditions, the eluting solvents are relatively polar and the stationary phase is non-polar in the reversed phase HPLC. Therefore, as a general rule, a solute that is more polar is expected to have a shorter elution time. The computed dipole moments indicate that the *R*-ETO derivative is more polar than the *S*-ETO derivative, and that the *R*-form is likely to elute ahead of the *S*-form. These results are consistent with those by *in vivo* assay. Therefore, it was concluded that the peaks 2 and 3 corresponded to the *R*- and *S*-ETO diastereomer, respectively.

3.4. Optimization of R-MCF derivatization conditions and the assessment of the derivatization reaction rates

Biological fluids usually require sample cleanup steps due to matrix complexity. In this study, protein precipitation method, which is one of the most popularly used methods, was used because it is simple and rapid. The two commonly used deproteination solvents, MeOH and ACN (Kole et al., 2011), both of which are easy to remove and have good dissolution capability for ETO, were tested, with the vortexing time fixed at three min to ensure complete mixing of serum and solvent. It was found that ACN yielded significantly higher total peak areas of the ETO derivatives than MeOH ($p < 0.001$) (Supplementary Fig. S4). As a result, ACN was used as the protein precipitation solvent in the subsequent experiments.

It was necessary to optimize the reaction conditions for *R*-MCF and ETO because previously published conditions employing *R*-MCF had only been established for reactions with amines, not carboxylic acids. A literature search and our own experiences with derivatization reactions involving chloroformate (Matzner et al., 1964; Lee et al., 2014) suggested that *R*-MCF derivatization could be affected by a number of variables, including the ratio of *R*-MCF to ETO and pyridine volume. Recently, alternative energy inputs such as microwave and ultrasound-assisted mixing have been proven to improve conventional organic synthesis (Baig and Varma, 2012). With regard to this, our preliminary experiments indicated that derivatization efficiency was significantly influenced by the external factor of whether and how contact between *R*-MCF and ETO was facilitated. Specifically, ultrasonic radiation of the reaction mixture was more efficient than incubation without agitation or vortexing for the same given period (data not shown). Thus, ultrasound-assisted derivatization was selected and the ultrasonic radiation time was included as a variable to be optimized while the ultrasonic power was set to maximum. In order to efficiently determine the optimal reaction conditions and explore the interactions between these variables, we applied RSM using a central composite design.

The following three variables were varied from the level of −1 to +1, and a sufficient volume of ACN was added to the reaction mixture to bring the final volume to 200 μL: (1) variable *A*, volume of 200 mM *R*-MCF (50–140 μL), (2) variable *B*, ultrasonic radiation time (5–18 min), and (3) variable *C*, pyridine volume (7–24 μL). The sum of the peak areas of *R*- and *S*- ETO derivatives was used as the response. The experimental design included 20 independent experiments

including 6 center points, 8 factorial points, and 6 axial points, and the experiments were performed in random order. As a result, the response was fitted to a polynomial quadratic equation using the coded factors as follows:

$$\text{Peak area} = +1080.31 + 258.07 \times A + 188.75 \times B + 113.94 \times C - 116.37 \times AB + 72.98 \times AC - 42.3 \times BC - 106.79 \times A^2 - 155.93 \times B^2 - 159.01 \times C^2$$

Based on the results of analysis of variance (ANOVA) (Supplementary Table S2), the constructed model was highly significant ($p = 0.0003$) with a satisfactory adjusted coefficient ($R^2_{adj} = 0.8639$). The regression model showed that all first-order and second-order terms for the three variables had significant coefficients. A negative interactive effect was observed between the *R*-MCF volume and ultrasonic radiation time. The results indicated that larger volumes of *R*-MCF and pyridine, and longer ultrasonic radiation time, generally contributed to higher peak areas of the diastereomers (Supplementary Fig. S5).

Based on the constructed model, the optimized conditions were determined to be 125 μL, 13 min, and 17 μL, for the *R*-MCF volume, ultrasonic radiation time, and pyridine volume, respectively. The derivatization reaction time of 13 min is much shorter than those by Jin et al. (2008) and Singh and et al. (1986) and it is comparable to or slightly longer than the reactions using (*S*)-anabasine (Higashi et al., 2012), (*R*)-(+)-α-methylbenzylamine (Singh and Bhushan, 2015). The derivatization was reproduced under these optimized conditions, and the resulting peak areas, 1180.6 (±90.7, $n = 3$), were found to be reasonably close to the predicted values (1244.8; 95% PI, 899.9–1589.6).

Under the optimized conditions, the reaction rates for *R*- and *S*-ETO were examined in the time course of derivatization reaction facilitated by ultrasonic radiation. As displayed in Fig. 3a, the derivatization reaction yields increased sharply for the beginning five min and continued to increase until 10 min, after which no significant changes were observed. EFs for *R*-ETO also reached the maximum after 10 min of reaction and remained unchanged thereafter (Fig. 3b). These results indicate that the reaction rate of *S*-ETO is faster than *R*-ETO in the beginning and that after 10 min of ultrasonic radiation, the reaction rates of the two enantiomers reached the steady state. At the optimal derivatization conditions of which the derivatization reaction time was 13 min, it can be inferred that the derivatization reaction rates were consistent. Consequently, the subsequent method development was conducted under these optimized conditions.

3.5. Salting-out assisted liquid–liquid extraction of the derivatives

After derivatization, 170 μL of aqueous L-proline solution was added to 200 μL of the reaction mixture to quench the reaction. This step introduced an unintended dilution of the sample and therefore decreased sensitivity. We adopted a salting-out assisted liquid–liquid extraction (SA-LLE) strategy to improve sensitivity (Farajzadeh et al., 2013; Wang et al., 2013). SA-LLE is performed by adding an electrolyte to an aqueous mixture to result in the phase separation between water-miscible organic solvent and water. SA-LLE has been widely applied to achieve increased analyte concentrations as well as sample cleanup (Valente et al., 2013; Wen et al., 2013). Specifically, we added NaCl to the quenched reaction mixture as a salting-out agent. Of various amounts tested from 0 to 20 mg, 20 mg of NaCl was found to be sufficient to readily induce phase separation of consistent volumes of the organic phase (data not shown). The derivatized products were found to be enriched in the resulting upper organic phase of more than 140 μL. While the entire SA-LLE procedure could be performed within less than 2 min, it helped achieve a relatively high sensitivity for ETO analysis in biological fluids.

3.6. Method validation

3.6.1. Specificity, sensitivity, and linearity

Specificity of the developed method was confirmed in the chromatograms of samples prepared from blank and spiked sera. No endogenous interfering peaks overlapped with the peaks of the ETO and IS derivatives (Fig. 2). The LOQ values measured based on the signal-to-noise ratio were 0.3 μg mL^{-1} for both *R*- and *S*-ETO. The linearity of the calibration curves that were established using spiked mouse sera was found to be in the range of 0.5–50.0 μg mL^{-1} for both enantiomers with

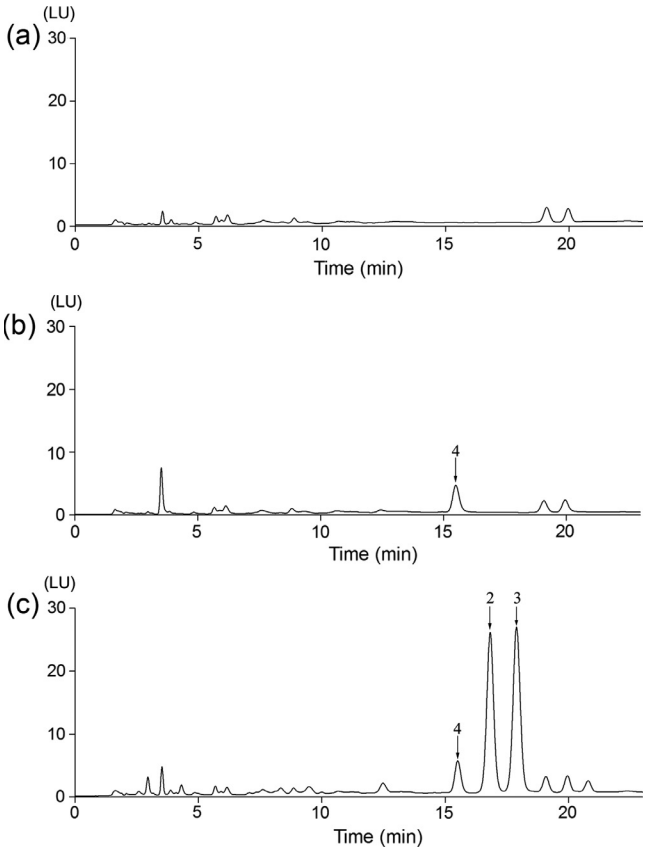

Figure 2 HPLC–FL chromatograms of samples prepared from blank serum (a), serum spiked with IS (b), and serum spiked with (±)-ETO and IS (c). The spiked concentrations for (±)-ETO and IS were 50.0 and 1.0 μg mL^{-1}, respectively. Peak identification: peaks 2, 3, and 4 correspond to compound 2 (ester derivative of *R*-ETO), 3 (ester derivative of *S*-ETO), and 4 (ester derivative of IS) in Fig. 1.

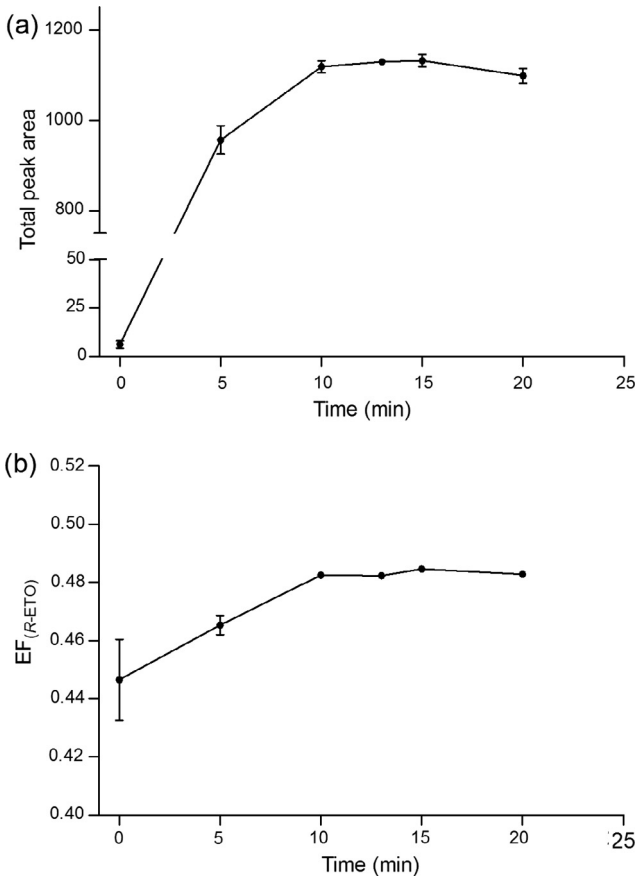

Figure 3 Total reaction yields of *R*- and *S*-ETO derivatives (a) and the enantiomeric fractions of the *R*-ETO derivative (b) in the time course of derivatization facilitated by ultrasound radiation. Error bars indicate the SEM ($n = 3$).

correlation coefficients (r^2) above 0.998. The parameters of the calibration curves are summarized in Table 3.

3.6.2. Precision and accuracy

The intra-day accuracy and precision for *R*-ETO were 96.2–99.8% and 2.2–6.2%, respectively, while the inter-day accuracy varied between 96.9% and 99.8% and the precision ranged from 1.9% to 6.1% (Table 4). In the case of *S*-ETO, the intra-day accuracy ranged between 97.0% and 108.7% while the precision ranged from 2.3% to 7.7%. The inter-day accuracy and precision for *S*-ETO were 97.9–107.8% and 2.2–7.8%, respectively. The quality of the intra- and inter-assay precisions and accuracies indicated that our method was suitable and reliable for analysis of the two enantiomers.

3.6.3. Stability

Stability of the *R*- and *S*-ETO derivatives was assessed using the QC samples at three different concentrations. *R*- and *S*-ETO were relatively stable in their derivative forms at 4 °C for at least 48 h (Supplementary Table. S3). These results show that the *R*-MCF ester derivatives are relatively stable, and suggest that the developed method may be applied for routine analysis of a number of clinical samples that cannot be analyzed in a single day.

3.6.4. Matrix effects

Although the matrix effect is generally a critical aspect of hyphenated MS techniques, it is also important to assess in the quantification methods for samples of complex matrices such as biological samples. In this study, the matrix effect was evaluated in two ways. The slope ratios of the external standard curves to the standard addition curves were determined to be 1.05 and 1.06 for *R*-ETO and *S*-ETO, respectively. Given that the slopes of the curves did not diverge (< 10% difference), it could be concluded that there was no matrix effect. Matrix effects (%) obtained from the peak area ratios of *R*- and *S*-ETO to IS in ACN and serum were 15.9%, 4.0%, and 5.5% at low, intermediate, and high concentrations, respectively, for *R*-ETO; 11.9%, 6.4%, and 5.9% at low, intermediate, and high concentrations, respectively, for *S*-ETO. Both results indicate that no significant matrix effects were evident.

3.7. Comparison of the developed method to other methods and application of the developed method

ETO has been analyzed by HPLC–UV in chiral quantification methods (Boni et al., 2000; Jin et al., 2008; Singh and Bhushan, 2015). In this study, we compared the two detection methods, UV and FL with respect to sensitivity and selectivity. In the chiral derivatization reaction, pyridine that was added as a catalyst was unavoidably retained in the sample after SA-LLE. Because pyridine has a strong UV absorbing property, its peak overwhelmed the HPLC–UV chromatograms at 226 nm that was the maximal absorption wavelength for the ETO diastereomers upon wavelength scanning. The LOQ values of the HPLC–UV method were 5.0 μg mL^{-1} for both *R*- and *S*-ETO, which is 17-fold higher than those of our developed method based on the FL detection. These results support that HPLC–FL analysis provides selective and sensitive determination of ETO enantiomers.

As summarized in Supplementary Table S4, the LOQ value of the current method (0.3 μg mL^{-1}) is comparable to or lower than those of other quantification methods for biological fluids, and this sensitivity was achieved using only 50 μL of sample volume. Specifically, the method reported by Hewala and et al. (2014) consumed 500 μL of plasma to obtain the LOQ values of 0.19–0.20 μg mL^{-1}, while slightly higher LOQ values than that of our method were achieved using a plasma volume of 150–200 μL (Jin et al., 2008). Although our method involves the derivatization procedure that may elongate the analysis time compared to direct chiral separation methods, its derivatization time is reasonably acceptable, and it is much

Table 3 Linearity and LOQ of the developed method.

Analyte	Calibration curve	r^2	Linear range (μg mL^{-1})	LOQ (μg mL^{-1})
R-ETO	$y = 0.1205x - 0.02000$	0.9987	0.5–50.0	0.3
S-ETO	$y = 0.1275x - 0.02207$	0.9991	0.5–50.0	0.3

Table 4 Intra- and inter-day assay accuracies and precisions.

Analyte	Concentration (μg mL^{-1})	Intra-assay (n = 5)		Inter-assay (n = 3 × 3)	
		Accuracy (%)	Precision (RSD%)	Accuracy (%)	Precision (RSD%)
R-ETO	0.5	98.4	6.2	96.9	6.1
	5.0	99.8	2.4	99.8	1.9
	50.0	96.2	2.2	97.0	3.3
S-ETO	0.5	108.7	7.7	107.8	7.8
	5.0	100.2	3.1	99.3	2.2
	50.0	97.0	2.3	97.9	3.4

shorter than that of the bioanalytical study reporting 2 h of chiral derivatization (Jin et al., 2008). In addition, our study applied the protein precipitation in combination with SA-LLE for sample cleanup and enrichment, which is simpler and more rapid than solid phase extraction (Hewala et al., 2014) or LLE (Becker-Scharfenkamp and Blaschke, 1993; Jin et al., 2008).

The developed method was applied to real serum samples taken from ICR mice administered (±)-ETO at a dose of 20 mg kg^{-1} by intraperitoneal injection (n = 3). The serum concentrations 30 and 60 min after administration were determined to be 26.7 and 13.9, 27.8 and 19.4, and 30.1 and 15.7 μg mL^{-1}, respectively, for *R*- ETO; and 2.4 and 1.2, 2.2 and 3.2, and 3.3 and 1.6 μg mL^{-1}, respectively, for *S*-ETO.

4. Conclusions

A simple and rapid sample preparation method involving the chiral derivatization of ETO using *R*-MCF, with the reaction facilitated by ultrasonic radiation and subsequent SA-LLE of the derivatives, was established via optimization of important variables of the derivatization reaction by RSM. This is the first report of enantioseparation by ultrasound-assisted diastereomer formation between the carboxylic acid group of enantiomers and *R*-MCF. The resulting stable ETO diastereomers could be baseline separated on a conventional C_{18} HPLC column under the simple optimized elution conditions. The SA-LLE, which enabled a very simple sample cleanup as well as concentration of the ETO derivatives, and the subsequent fluorescence detection of the derivatives, made the method selective and sensitive while consuming only 50 μL of serum. The validity of the developed method was demonstrated by successful application in the real serum sample analysis after ETO administration to several mice.

Acknowledgments

This study was supported by a Grant (No. 2011-0024225) from the Basic Science Research Program of the National Research Foundation of Korea (NRF), which is funded by the Ministry of Education, Science and Technology (MEST), Republic of Korea. LR and PR acknowledge the facilities for computations from the University of Mauritius.

Appendix A. Supplementary material

Supplementary data associated with this article can be found, in the online version, at http://dx.doi.org/10.1016/j.arabjc.2015.11.001.

References

Brocks, D.R., 2006. Drug disposition in three dimensions: an update on stereoselectivity in pharmacokinetics. Biopharm. Drug Dispos. 27 (8), 387–406.
Awad, H., El-Aneed, A., 2013. Enantioselectivity of mass spectrometry: challenges and promises. Mass Spectrom. Rev. 32 (6), 466–483.
McConathy, J., Owens, M.J., 2003. Stereochemistry in Drug Action. Prim. Care Companion J. Clin. Psychiat. 5 (2), 70–73.
Smith, S.W., 2009. Chiral toxicology: it's the same thing...only different. Toxicol. Sci. 110 (1), 4–30.
Shen, Q. et al, 2013. Stereoselective binding of chiral drugs to plasma proteins. Acta Pharmacol. Sin. 34 (8), 998–1006.
Tougou, K. et al, 2004. Stereoselective glucuronidation and hydroxylation of etodolac by UGT1A9 and CYP2C9 in man. Xenobiotica 34 (5), 449–461.
Lu, H., 2007. Stereoselectivity in drug metabolism. Expert. Opin. Drug Metab. Toxicol. 3 (2), 149–158.
Hewala, I.I. et al, 2014. Enantioselective HPLC–DAD method for the determination of etodolac enantiomers in tablets, human plasma and application to comparative pharmacokinetic study of both enantiomers after a single oral dose to twelve healthy volunteers. Talanta 130, 506–517.
Burke, D., Henderson, D.J., 2002. Chirality: a blueprint for the future. Br. J. Anaesth. 88 (4), 563–576.
Miller, C.P., Ullrich, J.W., 2008. A consideration of the patentability of enantiomers in the pharmaceutical industry in the United States. Chirality 20 (6), 762–770.
Evans, A.M., 1992. Enantioselective pharmacodynamics and pharmacokinetics of chiral non-steroidal anti-inflammatory drugs. Eur. J. Clin. Pharmacol. 42 (3), 237–256.
Boni, J.R. et al, 2000. Chiral bioequivalence. Effect of absorption rate on racemic etodolac. Clin. Pharmacokinet. 39 (6), 459–469.
Kolluri, S.K. et al, 2005. The R-enantiomer of the nonsteroidal antiinflammatory drug etodolac binds retinoid X receptor and induces tumor-selective apoptosis. Proc. Natl. Acad. Sci. USA 102 (7), 2525–2530.
Inoue, T. et al, 2010. R-etodolac induces E-cadherin and suppresses colitis-related mouse colon tumorigenesis. Oncol. Rep. 24 (6), 1487–1492.
Hardikar, M.S., 2008. Chiral non-steroidal anti-inflammatory drugs – a review. J. Indian Med. Assoc. 106 (9), pp. 615–618, 622, 624.
Stalcup, A.M., 2010. Chiral separations. Annu. Rev. Anal. Chem. (Palo Alto Calif) 3, 341–363.
de Pablos, R.R. et al, 2005. Separation of etodolac enantiomers by capillary electrophoresis. Validation and application of the chiral method to the analysis of commercial formulations. Electrophoresis 26 (6), 1106–1113.
Fanali, S., Catarcini, P., Presutti, C., 2003. Enantiomeric separation of acidic compounds of pharmaceutical interest by capillary electrochromatography employing glycopeptide antibiotic stationary phases. J. Chromatogr. A 994 (1–2), 227–232.

Becker-Scharfenkamp, U., Blaschke, G., 1993. Evaluation of the stereoselective metabolism of the chiral analgesic drug etodolac by high-performance liquid chromatography. J. Chromatogr. 621 (2), 199–207.

Ali, I., Aboul-Enein, H.Y., 2003. Enantioseparation of some clinically used drugs by HPLC using cellulose Tris (3,5-dichlorophenylcarbamate) chiral stationary phase. Biomed. Chromatogr. 17 (2–3), 113–117.

Ghanem, A. et al, 2010. Lipase-mediated enantioselective kinetic resolution of racemic acidic drugs in non-standard organic solvents: direct chiral liquid chromatography monitoring and accurate determination of the enantiomeric excesses. J. Chromatogr. A 1217 (7), 1063–1074.

Caccamese, S., 1993. Direct high-performance liquid chromatography (HPLC) separation of etodolac enantiomers using chiral stationary phases. Chirality 5 (3), 164–167.

Singh, N.N. et al, 1986. Stereoselective gas chromatographic analysis of etodolac enantiomers in human plasma and urine. J. Chromatogr. 382, 331–337.

Ogawa, S. et al, 2013. (S)-1-(4-dimethylaminophenylcarbonyl)-3-aminopyrrolidine: a derivatization reagent for enantiomeric separation and sensitive detection of chiral carboxylic acids by LC/ESI–MS/MS. J. Chromatogr. B Anal. Technol. Biomed. Life Sci. 940, 7–14.

Higashi, T. et al, 2012. Derivatization of chiral carboxylic acids with (S)-anabasine for increasing detectability and enantiomeric separation in LC/ESI–MS/MS. J. Sep. Sci. 35 (21), 2840–2846.

Jin, Y.X., Tang, Y.H., Zeng, S., 2008. Analysis of flurbiprofen, ketoprofen and etodolac enantiomers by pre-column derivatization RP-HPLC and application to drug-protein binding in human plasma. J. Pharm. Biomed. Anal. 46 (5), 953–958.

Singh, M., Bhushan, R., 2015. A novel approach for enantioseparation as applied to (RS)-etodolac from pharmaceutical formulations: LC MS and density functional theory support for confirmation of diastereomers so separated. Biomed. Chromatogr.

Christensen, E.B., Hansen, S.H., Rasmussen, S.N., 1995. Assay of tocainide enantiomers in plasma by solid-phase extraction and indirect chiral high-performance liquid chromatography after derivatization with (−)-menthyl chloroformate. J. Chromatogr. B Biomed. Appl. 670 (2), 243–249.

Koo, C. et al, 2012. Stereochemical analysis of methorphan using (−)-menthyl chloroformate. J. Forensic Sci. 57 (6), 1549–1555.

Paik, M.J., Nguyen, D.T., Kim, K.R., 2006. N-menthoxycarbonylation combined with trimethylsilylation for enantioseparation of beta-blockers by achiral dual-column gas chromatography. J. Chromatogr. A 1103 (1), 177–181.

Kino, R. et al, 2004. Remarkable effect of tris (4-fluorophenyl) phosphine oxide on the stabilization of chiral lanthanum complex catalysts. A new and practical protocol for the highly enantioselective epoxidation of conjugated enones. Org. Biomol. Chem. 2 (13), 1822–1824.

El Kousy, N.M., 1999. Spectrophotometric and spectrofluorimetric determination of etodolac and aceclofenac. J. Pharm. Biomed. Anal. 20 (1–2), 185–194.

Nam, M.W. et al, 2015. Enhanced extraction of bioactive natural products using tailor-made deep eutectic solvents: application to flavonoid extraction from Flos sophorae. Green Chem.

Polo-Diez, L.M. et al, 2015. Simultaneous enantiomeric determinations of acid and ester imidazolinone herbicides in a soil sample by two-dimensional direct chiral liquid chromatography. Talanta 144, 375–381.

Ribeiro, A.R. et al, 2014. Enantiomeric fraction evaluation of pharmaceuticals in environmental matrices by liquid chromatography–tandem mass spectrometry. J. Chromatogr. A 1363, 226–235.

Becke, A.D., 1993. Density-functional thermochemistry. III. The role of exact exchange. J. Chem. Phys. 98 (7), 5648–5652.

Lee, C., Yang, W., Parr, R.G., 1988. Development of the Colle–Salvetti correlation-energy formula into a functional of the electron density. Phys. Rev. B 37 (2), 785.

Zhao, Y., Truhlar, D.G., 2008. The M06 suite of density functionals for main group thermochemistry, thermochemical kinetics, noncovalent interactions, excited states, and transition elements: two new functionals and systematic testing of four M06-class functionals and 12 other functionals. Theor. Chem. Acc. 120 (1–3), 215–241.

Hehre, W.J. et al, 1986. In: Ab Initio Molecular Orbital Theory, vol. 67. Wiley, New York, et al.

Frisch, M., D Aniels, A.D., Farkas, Ö., Foresman, J.B., Ortiz, J.V., Cioslowski, J., Fox, D.J., 2009. Gaussian 09 (Revision D. 01), Gaussian. Inc., Wallingford CT

Cances, E., Mennucci, B., Tomasi, J., 1997. A new integral equation formalism for the polarizable continuum model: theoretical background and applications to isotropic and anisotropic dielectrics. J. Chem. Phys. 107 (8), 3032–3041.

Cossi, M. et al, 1996. Ab initio study of solvated molecules: a new implementation of the polarizable continuum model. Chem. Phys. Lett. 255 (4), 327–335.

Barone, V., Cossi, M., Tomasi, J., 1998. Geometry optimization of molecular structures in solution by the polarizable continuum model. J. Comput. Chem. 19 (4), 404–417.

Tomasi, J., Persico, M., 1994. Molecular interactions in solution: an overview of methods based on continuous distributions of the solvent. Chem. Rev. 94 (7), 2027–2094.

Food and Drug Administration, Guidance for Industry: Bioanalytical Method Validation, 2001. <http://www.fda.gov/downloads/drugs/guidancecomplianceregulatoryinformation/guidances/ucm070107.pdf>.

Sergi, M. et al, 2013. Micro extraction by packed sorbent coupled to liquid chromatography tandem mass spectrometry for the rapid and sensitive determination of cannabinoids in oral fluids. J. Chromatogr. A 1301, 139–146.

Chow, T.W. et al, 2011. A validated enantioselective assay for the simultaneous quantitation of (*R*)-, (*S*)-fluoxetine and (*R*)-, (*S*)-norfluoxetine in ovine plasma using liquid chromatography with tandem mass spectrometry (LC/MS/MS). J. Chromatogr. B Anal. Technol. Biomed. Life Sci. 879 (5–6), 349–358.

Matzner, M., Kurkjy, R.P., Cotter, R.J., 1964. The chemistry of chloroformates. Chem. Rev. 64 (6), 645–687.

Lee, C.H. et al, 2014. A new analytical method to determine nonsteroidal anti-inflammatory drugs in surface water using in situ derivatization combined with ultrasound-assisted emulsification microextraction followed by gas chromatography-mass spectrometry. Talanta 129, 552–559.

Farsam, H., Souri, E., Gharavi, N., 1999. A New HPLC technique for the separation of methocarbamol enantiomers*. J. Pharm. Pharmacol. 51 (7), 873–875.

Helmy, S.A., El-Bedaiwy, H.M., 2014. Validation of a liquid chromatography method for the simultaneous determination of several nonsteroidal anti-inflammatory drugs in human plasma for therapeutic drug monitoring. Ther. Drug Monit. 36 (1), 100–107.

Brocks, D.R., Jamali, F., 1990. The pharmacokinetics of etodolac enantiomers in the rat. Lack of pharmacokinetic interaction between enantiomers. Drug Metab. Dispos. 18 (4), 471–475.

Kole, P.L. et al, 2011. Recent advances in sample preparation techniques for effective bioanalytical methods. Biomed. Chromatogr. 25 (1–2), 199–217.

Baig, R.B., Varma, R.S., 2012. Alternative energy input: mechanochemical, microwave and ultrasound-assisted organic synthesis. Chem. Soc. Rev. 41 (4), 1559–1584.

Farajzadeh, M.A., Sheykhizadeh, S., Khorram, P., 2013. Salting-out homogeneous liquid–liquid extraction in narrow-bore tube: extraction and preconcentration of phthalate esters from water. J. Sep. Sci. 36 (5), 939–946.

Wang, Q., Yin, C.R., Xu, L., 2013. Optimization of hydrophilic interaction LC by univariate and multivariate methods and its

combination with salting-out liquid–liquid extraction for the determination of antihypertensive drugs in the environmental waters. J. Sep. Sci. 36 (6), 1007–1014.

Valente, I.M., Goncalves, L.M., Rodrigues, J.A., 2013. Another glimpse over the salting-out assisted liquid–liquid extraction in acetonitrile/water mixtures. J. Chromatogr. A 1308, 58–62.

Wen, Y. et al, 2013. Salting-out assisted liquid–liquid extraction with the aid of experimental design for determination of benzimidazole fungicides in high salinity samples by high-performance liquid chromatography. Talanta 106, 119–126.